A NEW METHOD FOR PREDICTING SITE-SPECIFIC WAVE-INDUCED HULL GIRDER LOADS ACTING ON SHIP-SHAPED OFFSHORE INSTALLATIONS IN BENIGN CONDITIONS

(Reference NO. IJME706, DOI No. 10.5750/ijme.v163iA4.14)

H J Kim, Department of Naval Architecture and Ocean Engineering at Pusan National University, South Korea; **M P Mujeeb-Ahmed**, Maritime Safety Research Centre, Department of Naval Architecture, Ocean & Marine Engineering at University of Strathclyde, UK; **J M Cabrera**, Department of Civil and Environmental Engineering at Universidad de las Américas Puebla, Mexico; and **J K Paik***, Department of Mechanical Engineering at University College London, UK; The International Centre for Advanced Safety Studies (Lloyd's Register Foundation Research Centre of Excellence, www.icass.center), South Korea
* Corresponding author. J K Paik (Email) j.paik@ucl.ac.uk

KEY DATES: Submitted: 06/04/21; Final acceptance: 27/01/22; Published 07/04/22

SUMMARY

The aim of this study is to develop a new method for predicting wave-induced hull girder loads acting on ship-shaped offshore installations in benign conditions. Unlike in trading ships, current classification society rules provide procedures to define the design values of wave-induced hull girder loads for ship-shaped offshore installations in survival conditions with site-specific metocean data considering that the installations always remain on site. However, ship-shaped offshore units with single-point or turret mooring systems can be disconnected to temporally evacuate from the fields during the severe storm. Also, some areas may be fully benign accommodating spread mooring systems. In these cases, their design wave-induced hull girder loads may be defined in a similar way to those of trading ships but associated with site-specific metocean data. This study proposes a probabilistic approach to determine the site-specific design values of wave-induced loads acting on ship-shaped offshore installations in benign conditions that also accounts for the effects of mooring system type. Six target regions – the North Sea, Gulf of Mexico, western coast of Africa, eastern coast of South America, south eastern coast of Asia and north western coast of Australia – were studied to compare the results corresponding to various sea states. A set of wave scenarios representing all possible wave events for each target region were selected using the Latin hypercube sampling technique. To demonstrate this method, the design values of the wave-induced vertical bending moments were determined for a very large crude oil carrier (VLCC)-class structure with a hypothetical floating, production, storage and offloading (FPSO) unit. The effects of the mooring system type (e.g., single-point mooring versus spread mooring) on the wave-induced hull girder loads of the ship-shaped offshore installations were also evaluated. A case study of the developed method was made by comparison with existing results in the literature and design values provided by classification society rules. The novelty of this study is associated with a new approach that can accurately determine wave-induced hull girder loads of ship-shaped offshore installations in benign conditions, taking into account the effects of site-specific ocean environmental conditions and mooring system type, and its main contribution to industry is to provide a practical technology for the safe and economical design of ship-shaped offshore hull structures.

1. INTRODUCTION

High structural strength is required to ensure safety and withstand loads acting on ship-shaped offshore structures; otherwise, the resulting damage can potentially lead to catastrophic accidents (Paik, 2020, 2022). Predicting the loads on hull girder structures is therefore critical for protecting life, property, and the environment in the marine industry. However, the determination of wave-induced hull girder loads, which is a paramount consideration in terms of ship-shaped structure types, is not straightforward due to the many uncertainties and complexities of ocean environmental conditions.

For these reasons, classification society rules provide effective guidelines to calculate design values of wave loads, considering survival conditions with the most probable extreme waves for a return period of 100 years as they are considered to always remain on the site for their lifetime. However, ship-shaped offshore installations with single-point or turret mooring systems can be disconnected if extreme environmental loads are imminent, sailed to sheltered areas and then returned to restart operation when the weather calms (Paik, 2022). In addition, a number of ship-shaped offshore installations with spread mooring systems are operating in fully benign environments such as western coast of Africa.

For such benign conditions, ship-shaped offshore units may not require taking into account survival conditions to determine wave-induced loads. By doing this, some attractive benefits are achieved in terms of safety and economy, such as lowering design loads, minimising structural scantlings, increasing cargo capacity, reducing risk to asset damage, making the production of lost infrastructure autonomous and eliminating the need of helicopter evacuations (Cabrera-Miranda et al., 2018; Daniel et al., 2013; Paik, 2018). Despite the

aforementioned advantages, current classification society rules provide extreme values of wave-induced hull girder loads in survival conditions only.

Previous studies have presented the evaluation of wave-induced loads on ship-shaped offshore installations. Sogstad (1995) proposed a simplified method to predict the wave-induced vertical bending moment during the early design stage. Hamdan (2003) analysed the factors affecting wave-induced loads on floating, production, storage, and offloading (FPSO) units. Guedes Soares et al. (2006) compared design values between numerical analysis validated by an experiment and DNV rules. Fonseca et al. (2010) compared wave-induced vertical bending moments obtained from experimental and numerical results under extreme wave conditions. Ivanov et al. (2011) discussed the probabilistic distribution of wave-induced bending moments and its effect on the total bending moment of FPSOs. Chen (2016) used a Weibull distribution to describe wave-induced bending moments for reliability analysis of stiffened panels on FPSOs. Cabrera-Miranda et al. (2018) used probabilistic scenario sampling and kriging metamodels to estimate exceedance diagrams for the wave-induced bending moments on FPSOs considering the disconnection during severe storms. Ozguc (2020) used sink-source theory to estimate wave-induced bending moments on a converted-tanker FPSO and discussed the effect of trading tanker services and FPSO services on the fatigue damage of the hull.

Table 1. Distribution of floating, production, storage, and offloading units (FPSOs) in primary oil and gas fields in 2021

Location	Operating FPSO	Percentage (%)
Worldwide	162	100
North Sea	20	12
Gulf of Mexico	5	3
Western coast of Africa	43	27
Eastern coast of South America	46	28
South eastern coast of Asia	22	14
North western coast of Australia	6	4

Although previous studies have provided estimates associated with wave-induced loads, all of the results in the literature were obtained considering survival conditions. Consequently, determining a practical value for ship-shaped offshore structures in benign conditions remains a challenge in the industry. This study aims to develop a method to determine the wave-induced hull girder loads for ship-shaped offshore installations in benign conditions. The method is based on a probabilistic approach associated with a limited number of credible scenarios, representing all possible events at a specific site. The scenarios are selected using the Latin hypercube sampling (LHS) technique (Paik, 2020; Ye, 1998).
A hypothetical FPSO representative of a ship-shaped offshore installation is used in this paper to demonstrate the proposed method. Six regions – the North Sea, Gulf of Mexico, western coast of Africa, eastern coast of South America, south eastern coast of Asia, and north western coast of Australia – are considered as the target locations for comparing the sea state results. The geographic distribution of FPSOs is listed in Table 1 (Boggs et al., 2021).

Wave-induced hull girder loads are affected by mooring systems (e.g., single-point mooring versus spread-point) due to the weathervane effect. Hence, the motion and load analysis are performed considering both the presence and absence of the weathervane effect.

2. PROCEDURE FOR DETERMINING THE SITE-SPECIFIC DESIGN VALUE OF WAVE-INDUCED HULL GIRDER LOADS

This section provides an overview of the procedure for determining wave-induced hull girder loads using a probabilistic approach (Paik et al., 2019; Paik, 2020), as outlined in Figure 1.

2.1 THREE-DIMENSIONAL FINITE ELEMENT MODELLING

The data associated with the principal dimensions, structural geometry, material properties, hull form, and loading conditions should be initially determined to define the target structure. Once the hull data are finalised, a three-dimensional finite model can be defined for analysing the motion and load.

2.2 PROBABILISTIC SELECTION OF WAVE SCENARIOS

Figure 2 illustrates the probabilistic method for selecting scenarios, representing all possible events. A number of parameters affect the site-specific sea state:

$$\text{Site-specific sea state} = f(X_1, X_2, \cdots, X_i, \cdots, X_n) \quad (1)$$

For efficient modelling, it is necessary to select the primary parameters that affect the wave-induced hull girder loads (Paik, 2020). Wave-induced hull girder loads are predominantly affected by waves. The following three dominant random parameters that affect the hull girder loads acting on ship-shaped offshore installations are considered here (Henriksen et al., 2008; Paik et al., 2019).

- X_1: Significant wave height, H_s
- X_2: Average zero-up-crossing wave period, T_z
- X_3: Wave direction, θ

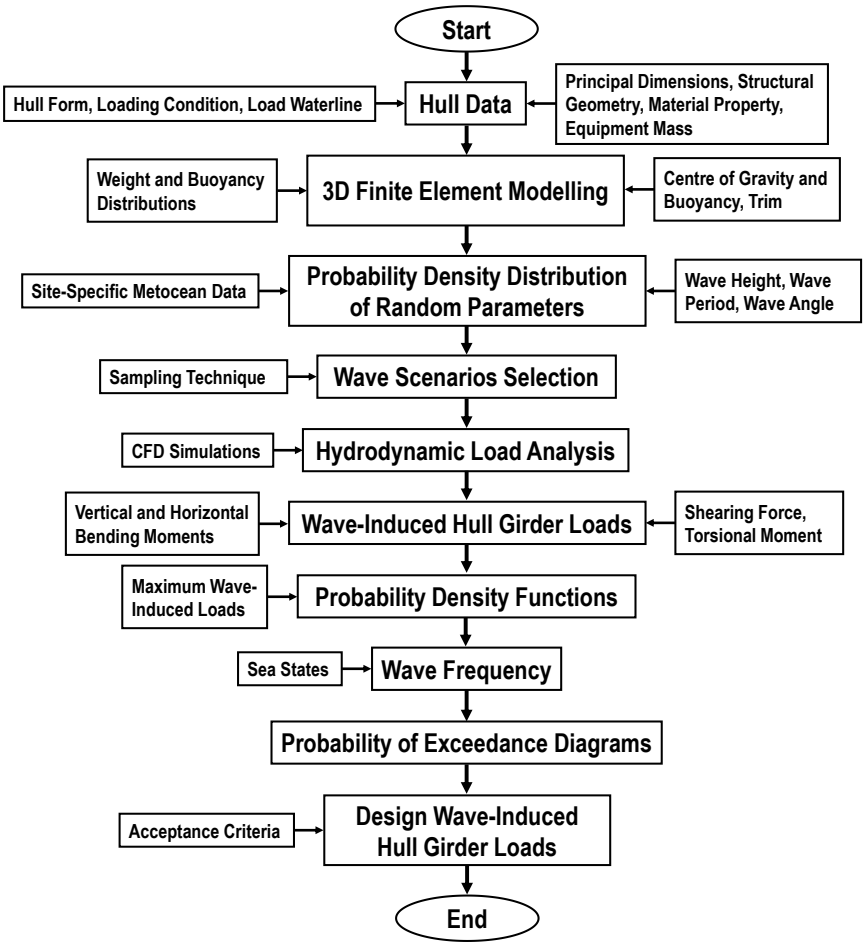

Figure 1. Proposed procedure for determining the design values of wave-induced hull girder loads on a ship-shaped offshore installation in benign conditions (where CFD = computational fluid dynamics)

Additional parameters (e.g., wind speed, wind direction, current speed, current direction) are available to refine the results (Cao et al., 2018).

After acquiring the parameter databases, the probability density function (PDF) for individual parameters can be defined to perform the scenario sampling. Several different types of PDFs are considered: two-parameter gamma; three-parameter gamma; normal; two-parameter log-normal; three-parameter log-normal; logistic; two-parameter log-logistic; three-parameter log-logistic; exponential; two-parameter exponential; two-parameter Weibull; and three-parameter Weibull functions. The best-fit PDF, which best represents the probabilistic parameter distribution, is determined using the goodness-of-fit (GoF) test.

The LHS technique is used to more effectively capture a limited number of scenarios. The probability of each sample generated by the LHS technique for n parameters can be obtained as (Paik, 2020):

$$P = \left(\frac{1}{m}\right)^n \tag{2}$$

where m is the number of scenarios.

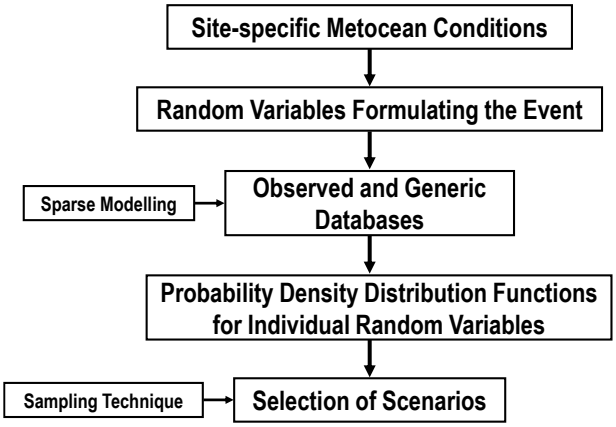

Figure 2. Probabilistic approach for selecting event scenarios (Paik, 2020)

2.3 MOTION AND LOAD ANALYSIS

A number of computer programs are available to analyse wave-induced motion and loads acting on ship-shaped offshore installations. As described in section 3, long-crested wave simulations are carried out using MAESTRO software based on linear frequency domain hydrodynamic strip theory using a 3-dimensional finite element model (Ma et al., 2012; Paik et al., 2019; Prini et al., 2018a, 2018b; Zhao et al., 2013; Zhao and Ma, 2016). The strip theory is an approximate method based on the potential flow theory for ship seakeeping calculation, providing good prediction for ship motions and hull girder loads. The ship motions and hull girder loads are determined by integrating the two-dimensional hydromechanics coefficients and wave exciting forces over the ship length.

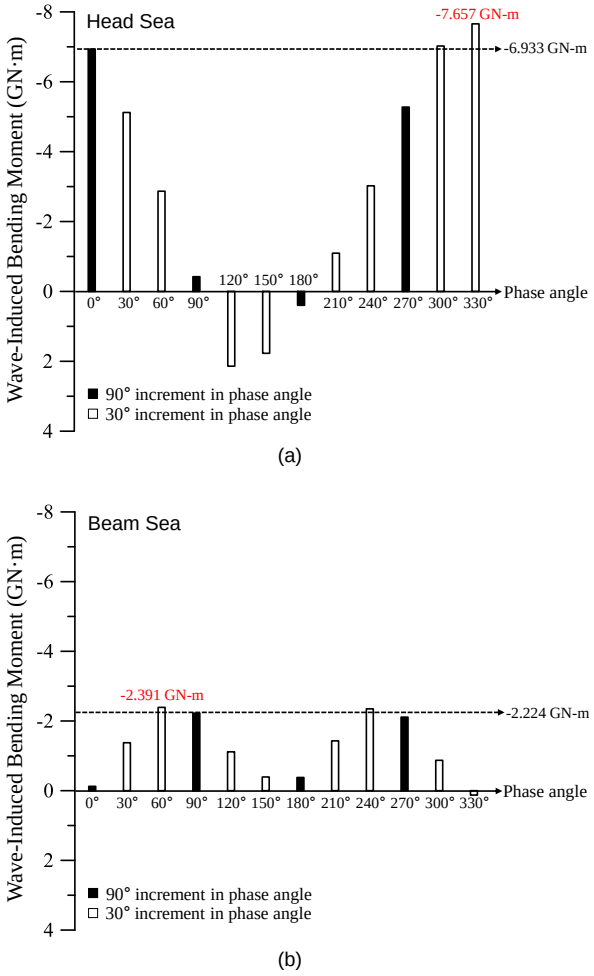

Figure 3. Wave-induced vertical bending moment by using 90° and 30° phase angle increment in H_s = 6m and T_z = 10s: (a) head sea; (b) beam sea

Wave-induced hull girder loads are determined for regular waves by varying phase angles while keeping the wave amplitude. From a screening analysis presented in Figure 3, it is observed that using a 90° phase angle step results in a good approximation compared to more refined 30° step. For the sake of computational efficiency and following Paik et al. (2019), four phase angles have been used in subsequent analyses, namely 0°, 90°, 180°, and 270°, which are considered to demonstrate the proposed method in section 3 as shown in Figure 4.

In order to determine the wave length, the following relationship is used (Chakrabarti, 2005):

$$\lambda = \frac{gT_z^2}{2\pi} \tag{3}$$

where λ is the wave length, T_z is the average zero-up-crossing wave period, and g is the gravitational acceleration (9.8 m/s^2).

2.4 DETERMINING THE SITE-SPECIFIC DESIGN VALUE OF WAVE-INDUCED HULL GIRDER LOADS

In the proposed method, the design values of the wave-induced hull girder loads are determined using the probability of exceedance. A probability of exceedance diagram is useful for the design value corresponding to the acceptable level of exceedance probability (Kristoffersen et al., 2021; Liu et al., 2016; Nubli and Sohn, 2021; Youssef et al., 2016; Zhao and Dong, 2020).

The probabilities of individual wave-event scenarios should be defined to establish the probability of exceedance diagrams. The probability of a wave scenario is defined as:

$$P_w = P_{hp} P_a \tag{4}$$

where P_w is the probability of a wave event, P_{hp} is the joint probability between a significant wave height and an average zero-up-crossing wave period, and P_a is the probability of the wave heading angle. P_a is defined as:

$$P_a = \frac{1}{N_a} P_a^* \tag{5}$$

where P_a^* is the occurrence probability of a given wave heading angle determined from the wave direction data and N_a is the occurrence number of the wave heading angle, which can be established from the wind direction changes. Setting a duration of 3 h for each sea state and 100 years for the return period, N_a can be defined as 100 × 365 × 24/3 = 292,000.

After the wave-induced hull girder loads corresponding to individual scenarios are obtained, the probability of exceedance diagram can be established as follows (Paik et al., 2019; Paik, 2020).

- Step 1: Establish a table of frequencies (probabilities) and wave-induced hull girder loads, including the highest loads of the different phase angles.

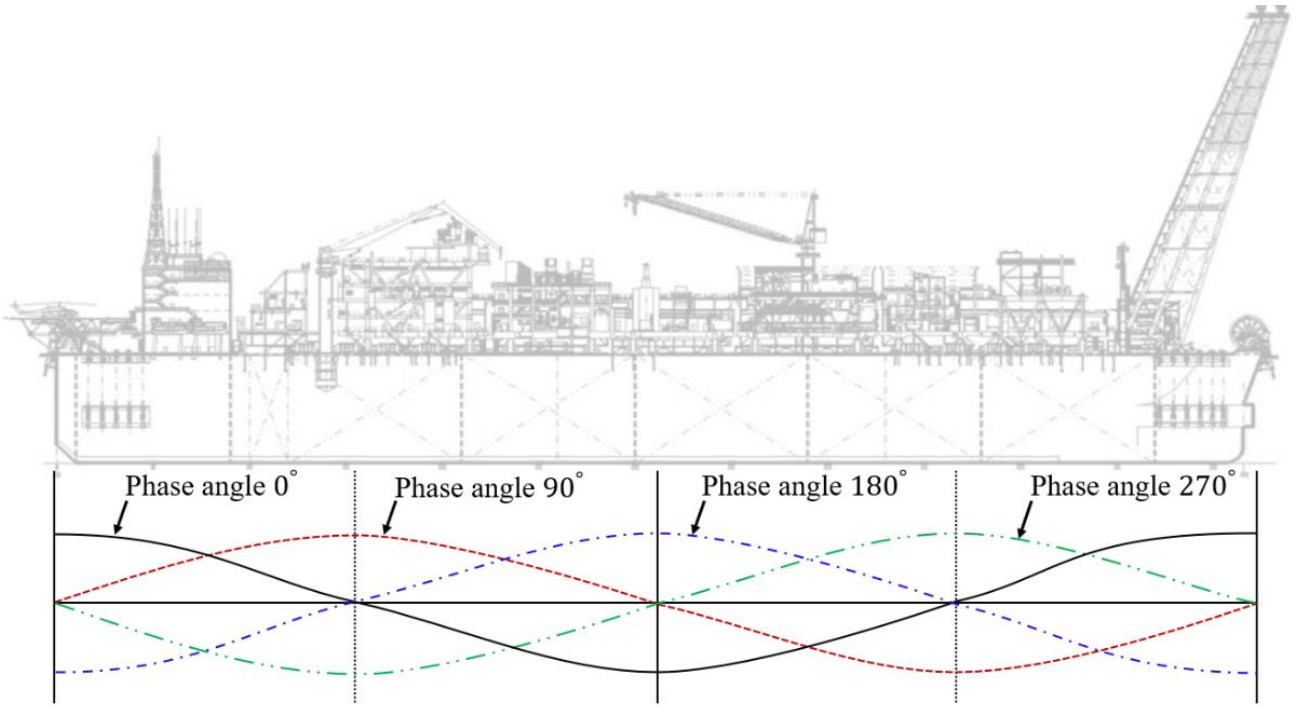

Figure 4. Four phase angles when the wave length equals the vessel length

- Step 2: Rearrange the order of scenarios so that the scenarios with the smallest and largest hull girder load become the first and last, respectively.

- Step 3: Calculate the cumulative probabilities (frequencies) from the bottom row associated with the largest hull girder load.

- Step 4: Determine the design value of the wave-induced hull girder load corresponding to an acceptable level of exceedance probability from the probability of exceedance diagram.

The acceptance level of the exceedance probability is defined using the expected number N_p of wave peaks during the design lifetime (100 years). If a wave peak occurs every 6–10 s, N_p is estimated as 100 × 365 × 24 × 60 × 60/10 = 315,360,000 or 100 × 365 × 24 × 60 × 60/6 = 525,600,000. Thus, the occurrence of the maximum wave peak is in the probabilistic range of 1.90×10^{-9} to 3.17×10^{-9} ($P = \frac{1}{N_p}$). In this regard, the design value of the hull girder loads can be calculated based on the lower end of the acceptance range (1.90×10^{-9}), which represents the most unfavorable load. The acceptance level of the exceedance probability presented here is a representative example, and it can be modified as more refined database becomes available.

3. APPLIED EXAMPLE

3.1 THREE-DIMENSIONAL FINITE ELEMENT FPSO MODEL FOR A VLCC-CLASS HYPOTHETICAL FPSO UNIT HULL

In this study, the data related to operating FPSOs built since 2000 were used to create a three-dimensional finite element model, as shown in Figure 5. Table 2 indicates the principal dimensions of the hypothetical FPSO model. The principal dimension ratio of the hypothetical FPSO model is similar to the results from a worldwide survey of newly built FPSOs conducted in 2021, as shown in Table 3. The weights at the topside and living quarters are assumed as 30,000 tons and 3,500 tons, respectively (Ha et al., 2016, 2017; Hwang et al. 2010). FPSOs are generally subjected to severe hull girder loads under fully loaded conditions. Thus, a hypothetical FPSO under fully loaded conditions was assumed for the wave simulations.

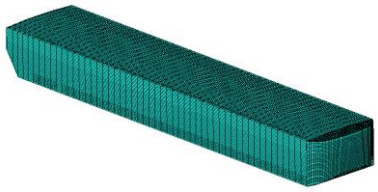

(a)

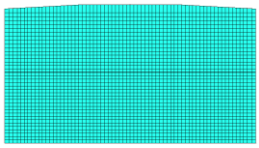

(b)

(c)

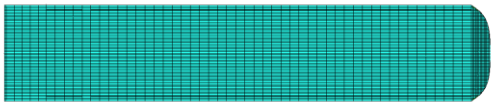

(d)

Figure 5. Three-dimensional finite element model of the hypothetical floating, production, storage, and offloading unit hull: (a) overall view; (b) body plan view; (c) profile view; (d) plan view

Table 2. Principal dimensions of the hypothetical floating, production, storage, and offloading unit model

Parameter	Dimension
Length Between Perpendiculars (L)	305.0 m
Breadth (B)	60.0 m
Depth (D)	32.0 m
Design Draught (T)	23.3 m
Block Coefficient (C_b)	0.975

In addition, DNV (2019) provides worldwide wave scatter diagrams expressed by a two-parameter Weibull distribution for significant wave height and log-normal distribution for average zero-up-crossing wave periods. However, this may be less accurate than the best-fit distribution corresponding to the historical wave data because DNV gives the worldwide sea states using only one distribution type for each parameter.

Table 3. Comparison of the principal dimension ratios between average values of worldwide floating, production, storage, and offloading units (FPSOs) and the hypothetical FPSO (Boggs et al., 2021)

Type	*L/B*	*B/D*	*T/D*	*B/T*
Newly-built FPSO worldwide	5.1	1.9	0.7	2.8
Hypothetical FPSO	5.1	1.9	0.7	2.6

Table 4. Specific locations of the target regions based on the floating, production, storage, and offloading units (FPSOs) in service

Site	Target FPSO	Latitude	Longitude
North Sea	PETROJARL KNARR	61.78°N	2.83°E
Gulf of Mexico	YÙUM K'AK' NÁAB	19.60°N	92.30°W
Western coast of Africa	EGINA	3.05°N	6.70°E
Eastern coast of South America	PETROBRAS67	25.33°S	42.69°W
South eastern coast of Asia	PFLNG SATU	6.45°N	115.44°E
North western coast of Australia	PRELUDE	13.79°S	123.31°E

3.2 SCENARIO SELECTION

3.2 (a) Site-specific sea states

Six target regions were selected, as described in section 1. The exact locations of the actual FPSOs in service were used in this study. Table 4 provides the specific latitudes and longitudes of the target FPSOs. Historical wave data from 1979 to 2019 were derived from the DHI MetOcean Data Portal (https://www.metocean-on-demand.com, accessed 29 January 2021), where a spectral wave model known as MIKE 21 is used to predict site-specific wave characteristics (DHI, 2019).

3.2 (b) Probability density functions

The PDF must be defined to select wave scenarios. To determine the best-fit distributions, the Anderson-Darling test is applied for the GoF (Abyani et al., 2018). Table 5 depicts the best-fit distributions of the six regions for the significant wave height, average zero-up-crossing wave period, and wave heading angle determined by one of the following two PDF types (Paik, 2022).

Weibull distribution:

$$f(x) = \frac{C_2}{C_1}\left(\frac{x-C_3}{C_1}\right)^{C_2-1} \exp\left[-\left(\frac{x-C_3}{C_1}\right)^{C_2}\right] \qquad (6)$$

where C_1 is the scale parameter, C_2 is the shape parameter, and C_3 is the location parameter.

Log-normal distribution:

$$f(x) = \frac{1}{x\sqrt{2\pi}C_2} \exp\left[-\frac{(\ln x - C_1)^2}{2C_2^2}\right], \; x > 0 \qquad (7)$$

where C_1 is the mean and C_2 is the standard deviation.

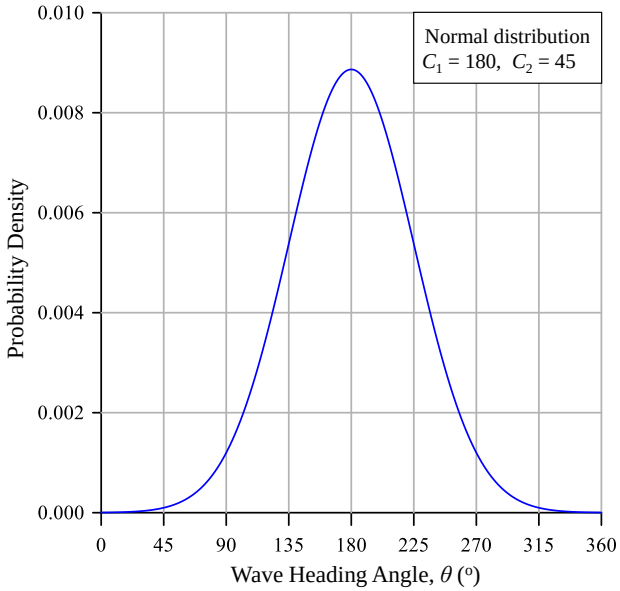

Figure 6. Probability density function of a wave heading angle for a turret mooring with the weathervane effect

The wave heading angle is defined by the site-specific wind direction in this paper because wave direction closely correlates with wind direction (Fontaine et al., 2013; Olsen et al., 2006; Sha et al., 2018). To evaluate the effects of the mooring system on the hull girder loads, different PDFs of wave heading angles were used to select the wave scenarios. The PDFs of a spread mooring without the weathervane effect are defined by the site-specific wind direction data. In contrast, the PDF of a turret mooring with the weathervane effect are defined following the normal distribution, thus the hypothetical FPSO primarily experiences head sea conditions, as shown in Figure 6 (Zangeneh et al., 2017; Zhao et al., 2012).

$$f(x) = \frac{1}{\sqrt{2\pi}C_2} \exp\left[-\frac{(x-C_1)^2}{2C_2^2}\right] \tag{8}$$

where C_1 = 180 and C_2 = 45.

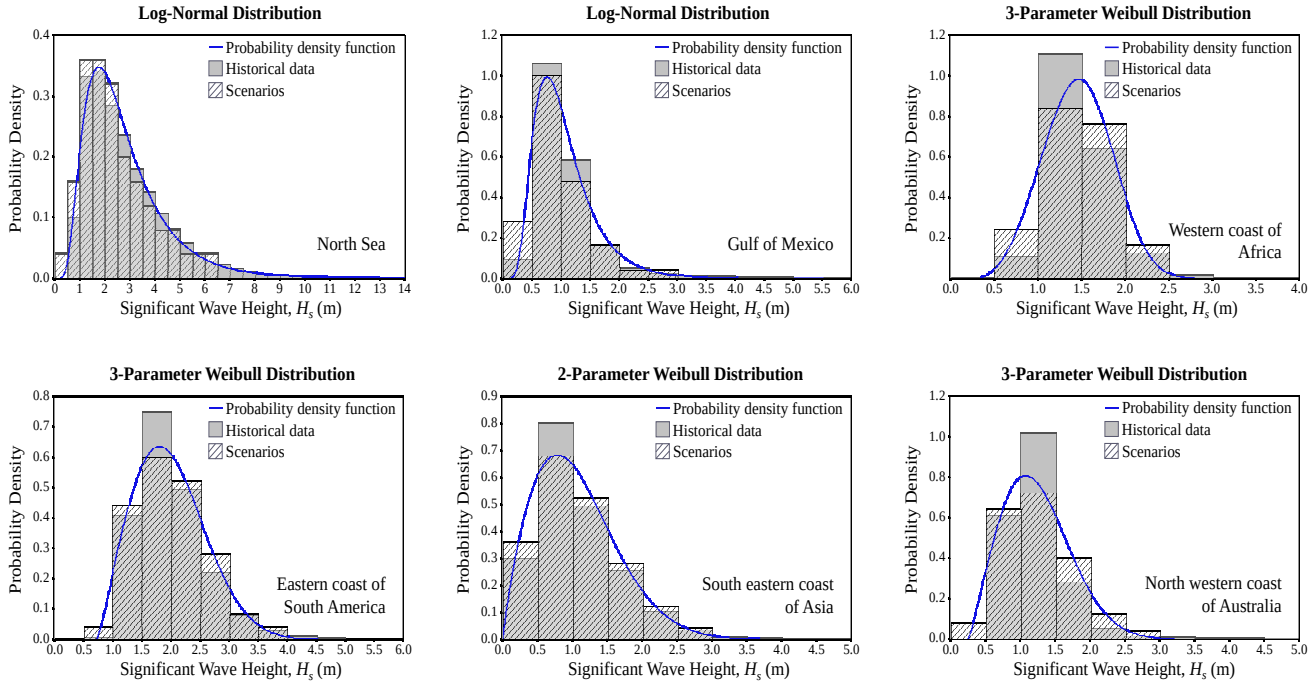

(a)

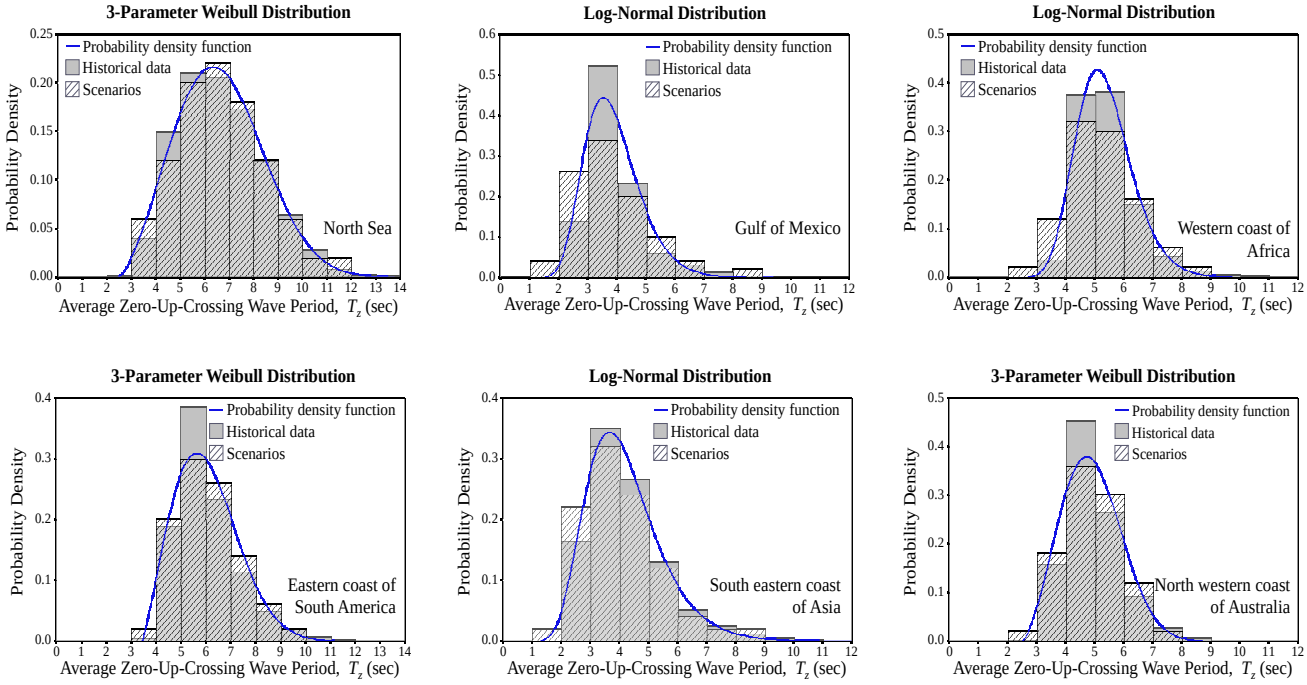

(b)

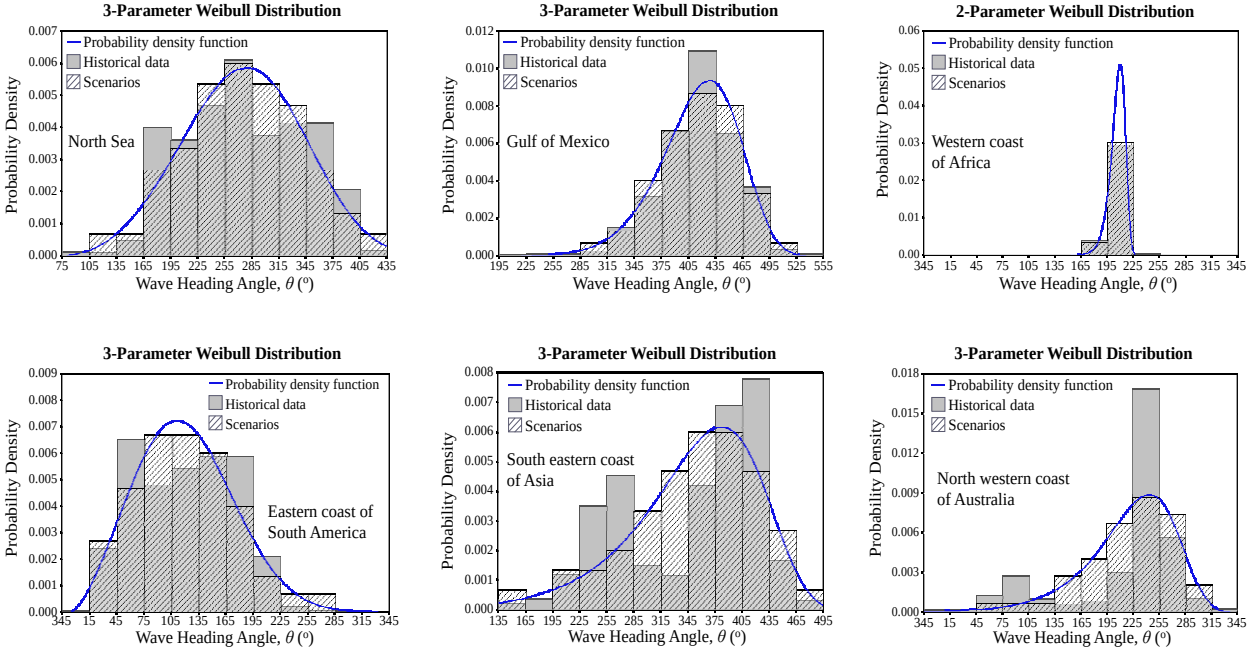

(c)

Figure 7. Selected scenarios with the historical and best-fit PDF for six operational regions: (a) significant wave height; (b) average zero-up-crossing wave period; (c) wave heading angle

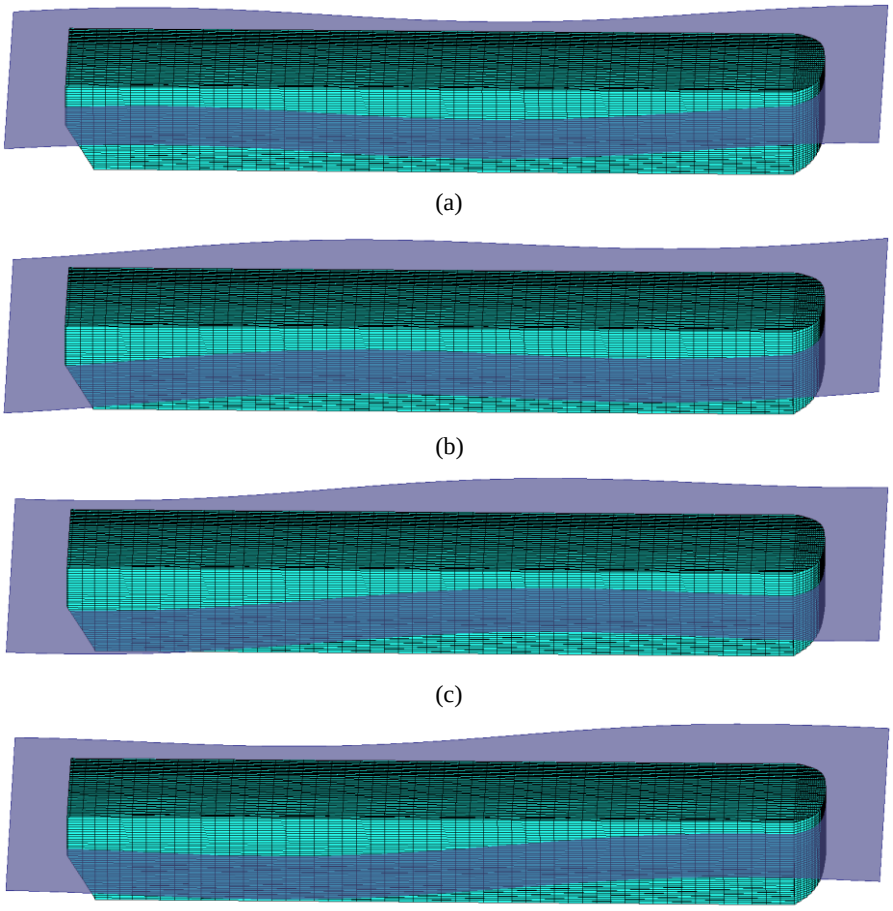

(a)

(b)

(c)

(d)

Figure 8. Four phase angles in the MAESTRO software: (a) 0°; (b) 90°; (c) 180°; (d) 270°

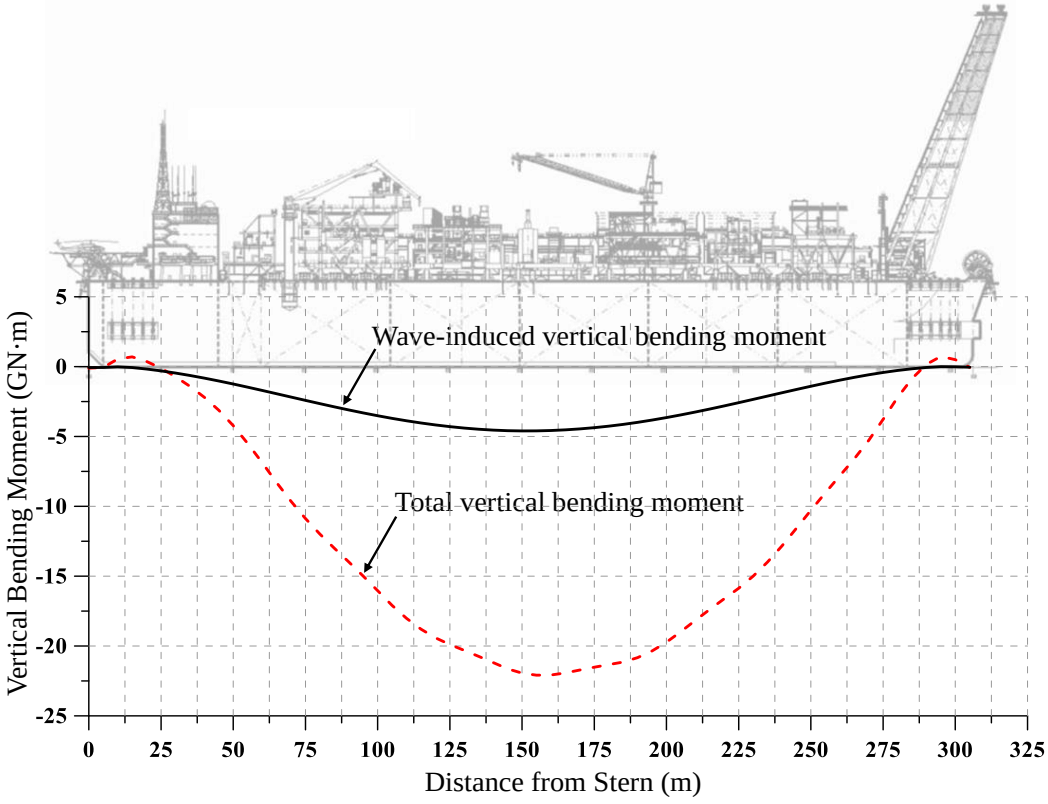

(a)

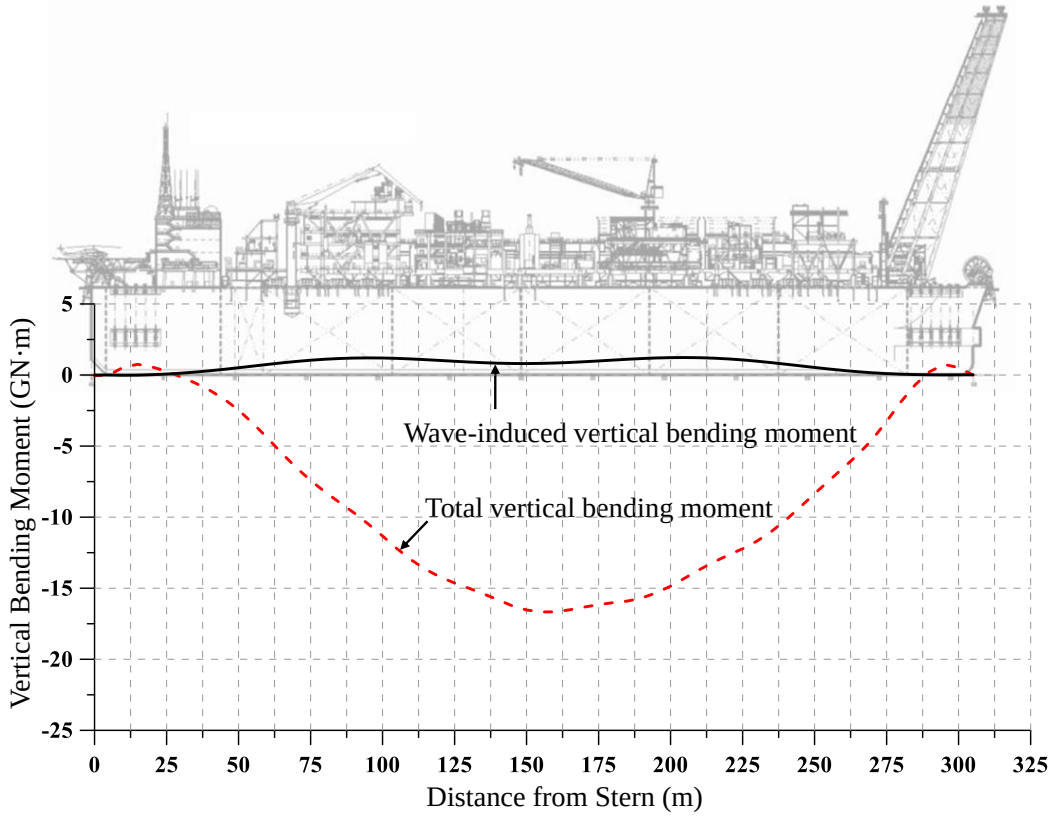

(b)

Figure 9. Distribution of total and wave-induced vertical bending moments of the hypothetical FPSO hull: (a) scenario 23 in the North Sea; (b) scenario 29 in the western coast of Africa

3.2 (c) Scenarios selection

Fifty wave scenarios are selected with the LHS technique using the marginal PDFs, as depicted in Figure 7. In general, FPSOs with spread moorings are also installed to generate head sea conditions as much as possible (Xu et al., 2019). For this reason, the wave heading angle in the spread mooring scenarios are adjusted to achieve the highest probability of the wave heading angle for head seas (180°). Some PDFs representing the wave heading angle are greater than 360° in Figure 7; thus 360° must be subtracted.

3.3 MOTION AND LOAD ANALYSIS

Wave-induced hull girder loads consist of different load types including the vertical bending moment, horizontal bending moment, torsional moment, and shearing force (Gaspar et al., 2016; Rörup et al., 2017; Tanaka et al., 2015). In this paper, the design value of the vertical bending moment is selected as an example of the proposed method. The design values of the other hull girder loads can be determined following identical processes.

MAESTRO software is used for the hydrodynamic analysis. Figure 8 shows four phase angles considered in the MAESTRO computations, as described in section 2.3. Only vertical bending moments at the midship region ($0.3L \leq x \leq 0.7L$) are considered in the results, where L is the ship length. Figure 9 shows the total vertical bending moment and wave-induced vertical bending moment of the hypothetical FPSO model. The total bending moment is the sum of the still-water bending moment and wave-induced bending moment.

4. SITE-SPECIFIC DESIGN VALUES OF THE WAVE-INDUCED VERTICAL BENDING MOMENT

4.1 PROBABILITY OF WAVE SCENARIOS

The probability of a wave event is defined from Eq. (4). To consider the interacting effects between the significant wave height and zero-up-crossing wave period, P_{hp} can be calculated using interpolation or extrapolation of a site-specific wave scatter diagram as a joint probability. To estimate the probability of exceedance diagram, the cumulative probabilities should be calculated using steps 2 and 3 in section 2.4.

4.2 WAVE-INDUCED HULL GIRDER LOADS

The design values of the wave-induced vertical bending moments are determined using the probability of exceedance diagrams, as shown in Figure 10. The resulting design values are presented in Table 6, which are calculated based on the lower acceptance range of the probability of exceedance, i.e., 1.90×10^{-9} (see section 2.4). All of the design vertical bending moments obtained are negative values because FPSOs are generally deployed in sagging conditions.

Table 5. Best-fit distribution with wave parameter coefficients for the six investigated regions

Location	Significant wave height				Average zero-up-crossing wave period				Wave heading angle			
	PDF	C_1	C_2	C_3	PDF	C_1	C_2	C_3	PDF	C_1	C_2	C_3
North Sea	Lognormal	0.874	0.561	-	Weibull	4.732	2.545	2.441	Weibull	238.3	3.634	61.33
Gulf of Mexico	Lognormal	-0.055	0.474	-	Lognormal	1.323	0.246	-	Weibull	310.3	7.830	123.5
Western coast of Africa	Weibull	1.347	3.440	0.243	Lognormal	1.660	0.181	-	Weibull	210.2	29.06	-
Eastern coast of South America	Weibull	1.428	2.172	0.722	Weibull	2.921	2.155	3.451	Weibull	142.7	2.562	-6.438
South eastern coast of Asia	Weibull	1.191	1.836	-	Lognormal	1.388	0.303	-	Weibull	5666	95.02	-5283
North western coast of Australia	Weibull	1.111	2.139	0.249	Weibull	2.718	2.566	2.478	Weibull	11481	277.2	-11237

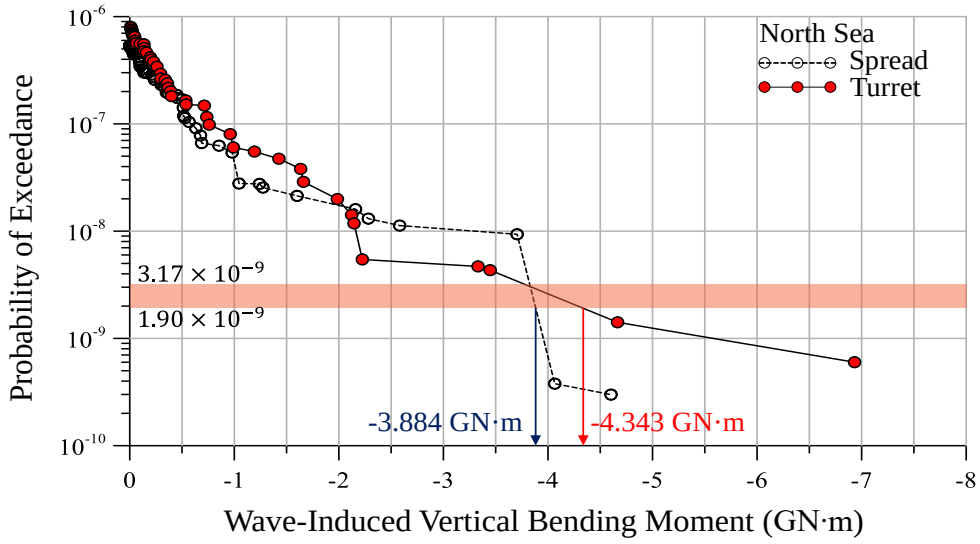

(a)

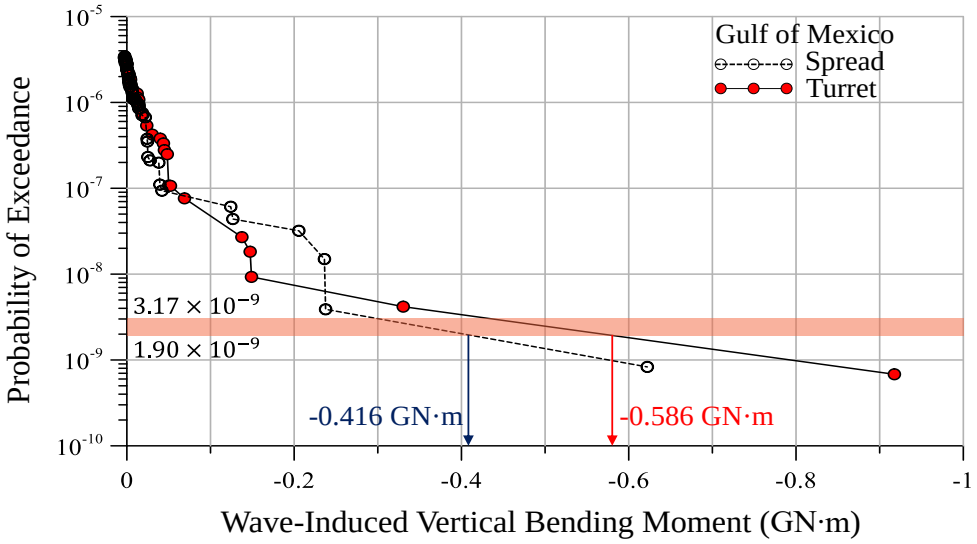

(b)

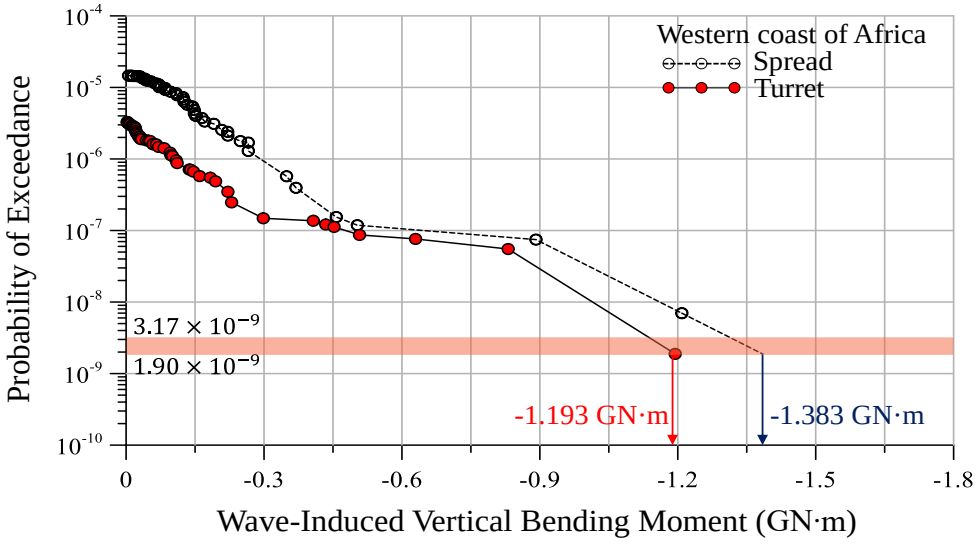

(c)

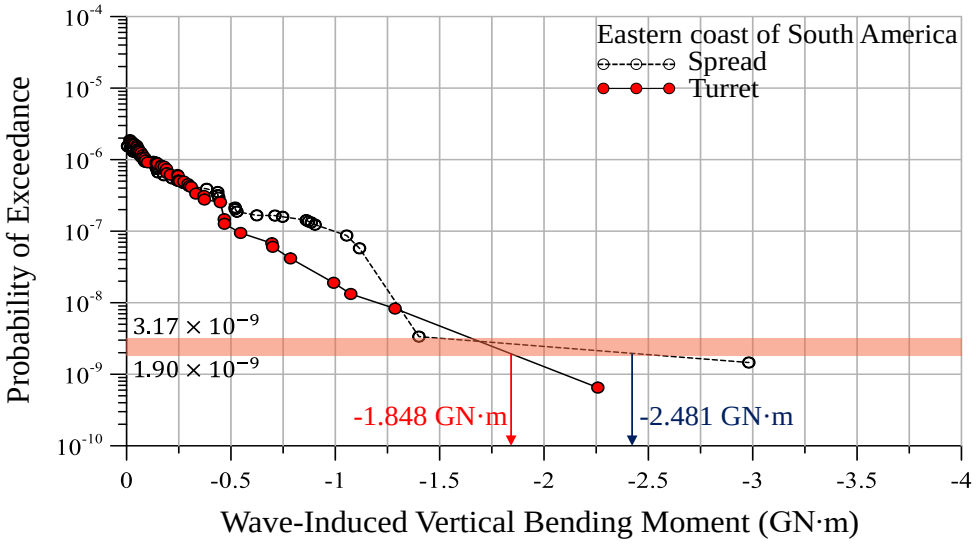

(d)

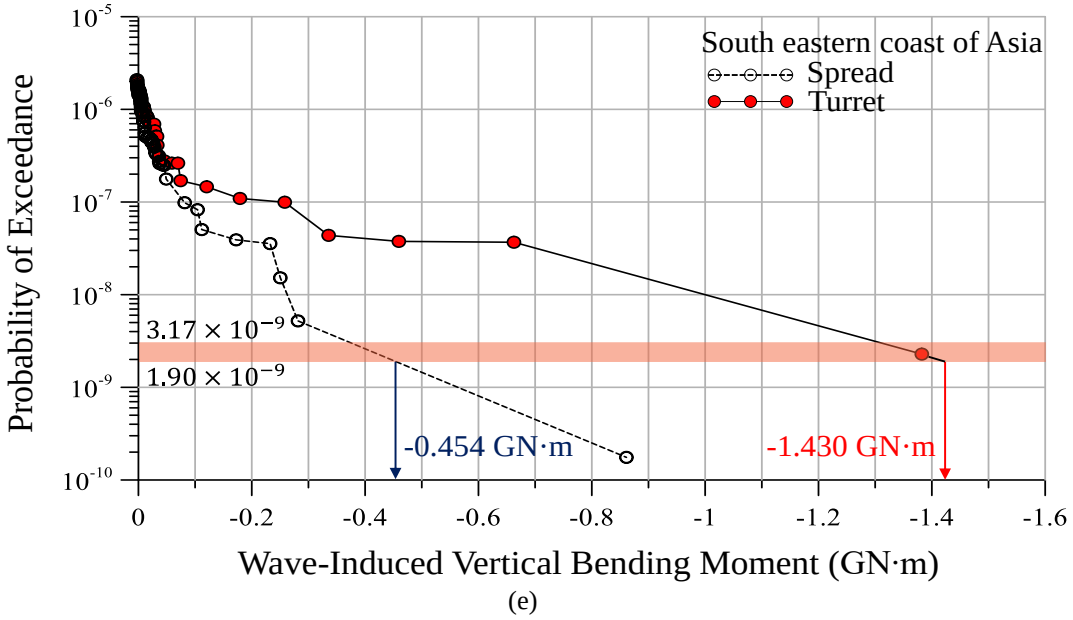

(e)

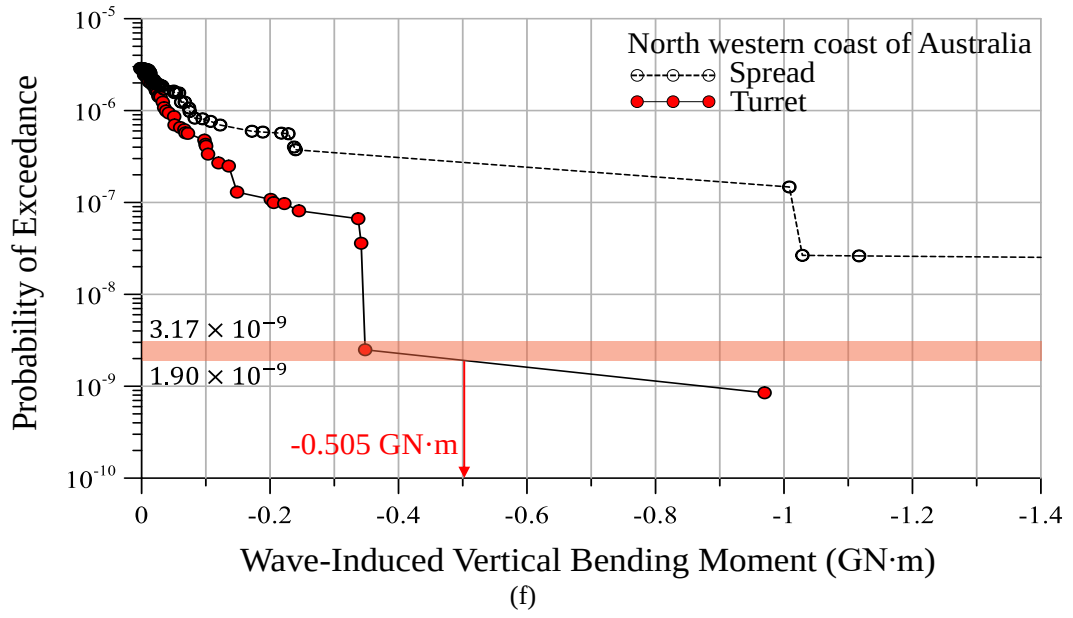

(f)

Figure 10. Probability of exceedance diagrams of the wave-induced vertical bending moment: (a) North Sea; (b) Gulf of Mexico; (c) Western coast of Africa; (d) Eastern coast of South America; (e) South eastern coast of Asia; (f) North western coast of Australia

Table 6. Design values of wave-induced vertical bending moment

Location	Spread mooring (GN·m)	Turret mooring (GN·m)
North Sea	−3.884	−4.343
Gulf of Mexico	−0.416	−0.586
Western coast of Africa	−1.383	−1.193
Eastern coast of South America	−2.481	−1.848
South eastern coast of Asia	−0.454	−1.430
North western coast of Australia	-	−0.505

Table 7. Comparison of wave-induced vertical bending moment between the present method and the existing results

Method		$L \times B \times D / T$ (m)	C_b	WBM (GN·m)	α_L	Scaled WBM (α_L^4 WBM) (GN·m)	Remark
Present	A	305.0 × 60.0 × 32.0/23.3	0.975	−4.34	1.00	-4.34	Figure 1
Sogstad (1995)	B	200.6 × 36.8 × 20.8/14.0	0.84	−4.05	1.52	-21.64	Linear strip theory
	C	227.6 × 44.0 × 26.6/15.2	0.83	−5.72	1.34	-18.45	Linear strip theory
	D	242.0 × 41.0 × 25.0/18.7	0.79	−6.12	1.26	-15.44	Linear strip theory
Maerli et al. (2000)	E	233.0 × 42.0 × 21.3/14.7	-	−3.05	1.31	-8.96	Linear strip theory
Guedes Soares et al. (2006)	F	259.8 × 46.0 × 27.0/16.7	0.87	−7.30	1.17	-13.87	Linear long-term prediction
	G	259.8 × 46.0 × 27.0/16.7	0.87	−8.10	1.17	-15.39	Nonlinear transfer function
	H	3.47 × 0.6 × 0.3/0.2	0.87	−5.10	1.17	-9.69	1/81-scaled physical model testing in the wave tank

where L = length between perpendiculars; B = breadth; D = depth; T = design draught; C_b = block coefficient; and WBM = wave-induced bending moment; α_L = length scale factor.

The results show that the proposed method effectively determines the design value depending on the site-specific sea state. Figure 11 compares the design values for ship-shaped offshore installations under the sea states of the six investigated regions. As expected, the maximum wave-induced bending moment is observed in the North Sea due to prevailing harsh environmental conditions.

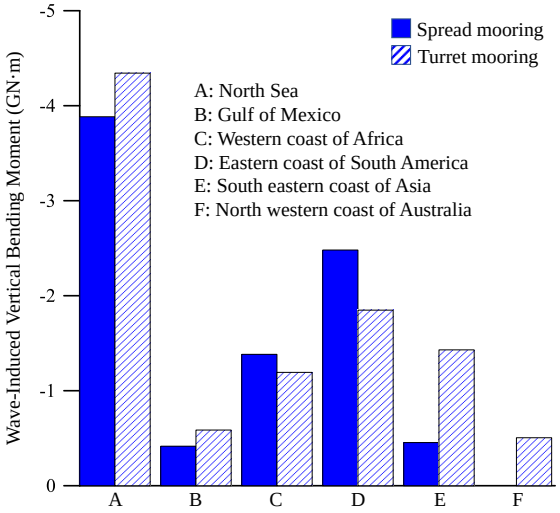

Figure 11. Comparison of the design values for ship-shaped offshore installations under the sea states of the investigated six regions

A comparison of the proposed method with different results considering survival conditions for FPSO unit hulls in the North Sea are presented in Figure 12. The results of B to H were obtained in the literature and scaled up corresponding to the length of a hypothetical FPSO based on Froude scaling laws. Hull dimensions and method for hydrodynamic analysis of those studies are indicated in Table 7. There are of course considerable differences, since the proposed method aims to predict the design value of wave-induced hull girder loads in benign conditions, while the existing results of B to H were obtained considering survival conditions.

The results of I to L were calculated by classification society rules of ABS (2021), BV (2016), DNV (2021) and LR (2021), respectively. The rules provide procedures for direct hydrodynamic analysis, and equations based on environmental factors and the IACS Common Structure Rules (CSR) to determine the design value of wave loads (IACS, 2021). Table 8 and Figure 13 indicates a comparison of the present method with the classification society rules for the six investigated regions. As expected, the present method solutions are greatly smaller than the rule results. This is because that the classification society rules estimate the extreme values of wave-induced hull girder loads for survival conditions, while the present method calculates the design values for benign conditions considering that single-point or turret mooring systems are disconnected if extreme environmental loads are imminent, sailed to sheltered areas and then returned to restart operation when the weather calms.

The proposed method can also be used to determine a suitable mooring system in terms of the wave-induced hull girder loads. For the spread mooring case on the north western coast of Australia, the design wave-induced bending moment becomes infinite and cannot be determined from the probability of exceedance diagram. However, a few design values do not match with the mooring type distribution at the sites. This is because the determination of the mooring system is affected not only by the wave-induced loads but also other variables, such as the stability of the ship motion and riser.

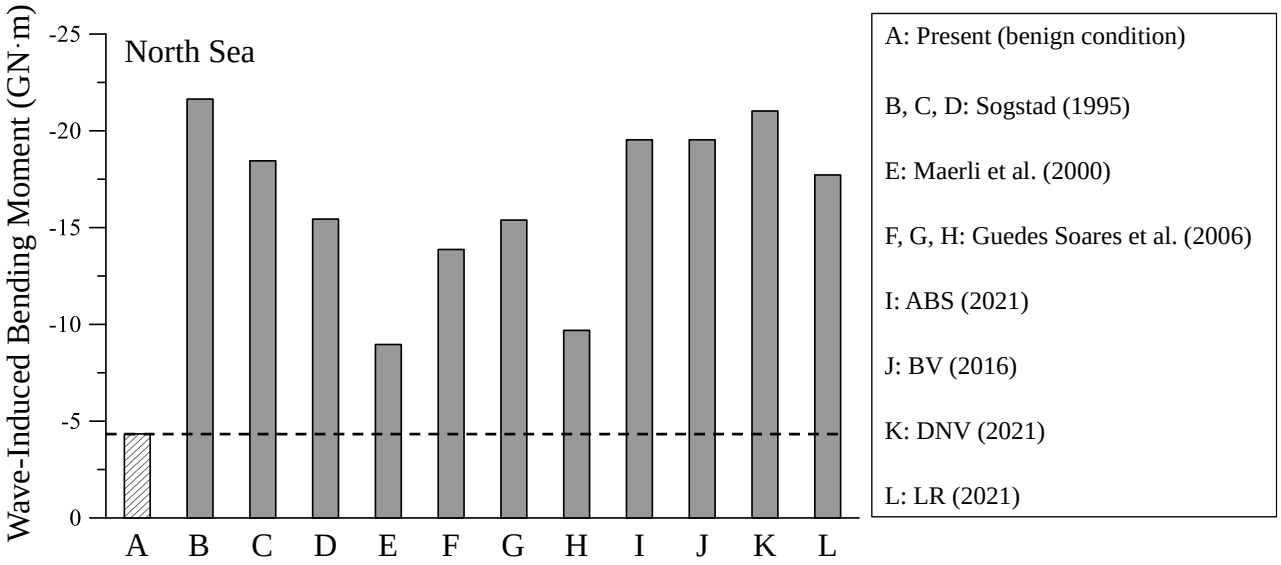

Figure 12. Comparison of the wave-induced vertical bending moments between the present method and the existing results in survival conditions for FPSO unit hulls in the North Sea

Table 8. Comparison of the design wave-induced vertical bending moments between the present method and classification society rules for the six investigated regions

	Design Wave-induced Vertical Bending Moments (GN·m)				
Location	Present	ABS (2021)	BV (2016)	DNV (2021)	LR (2021)
North Sea	-4.343	-19.536	-19.536	-21.025	-17.720
Gulf of Mexico	-0.586	-9.414	-9.950	-11.075	-5.538
Western coast of Africa	-1.138	-9.414	-8.844	-11.075	-5.538
Eastern coast of South America	-2.481	-9.414	-8.844	-11.075	-6.645
South eastern coast of Asia	-1.430	-9.414	-8.844	-11.075	-5.538
North western coast of Australia	-0.505	-9.414	-9.950	-11.075	-5.538

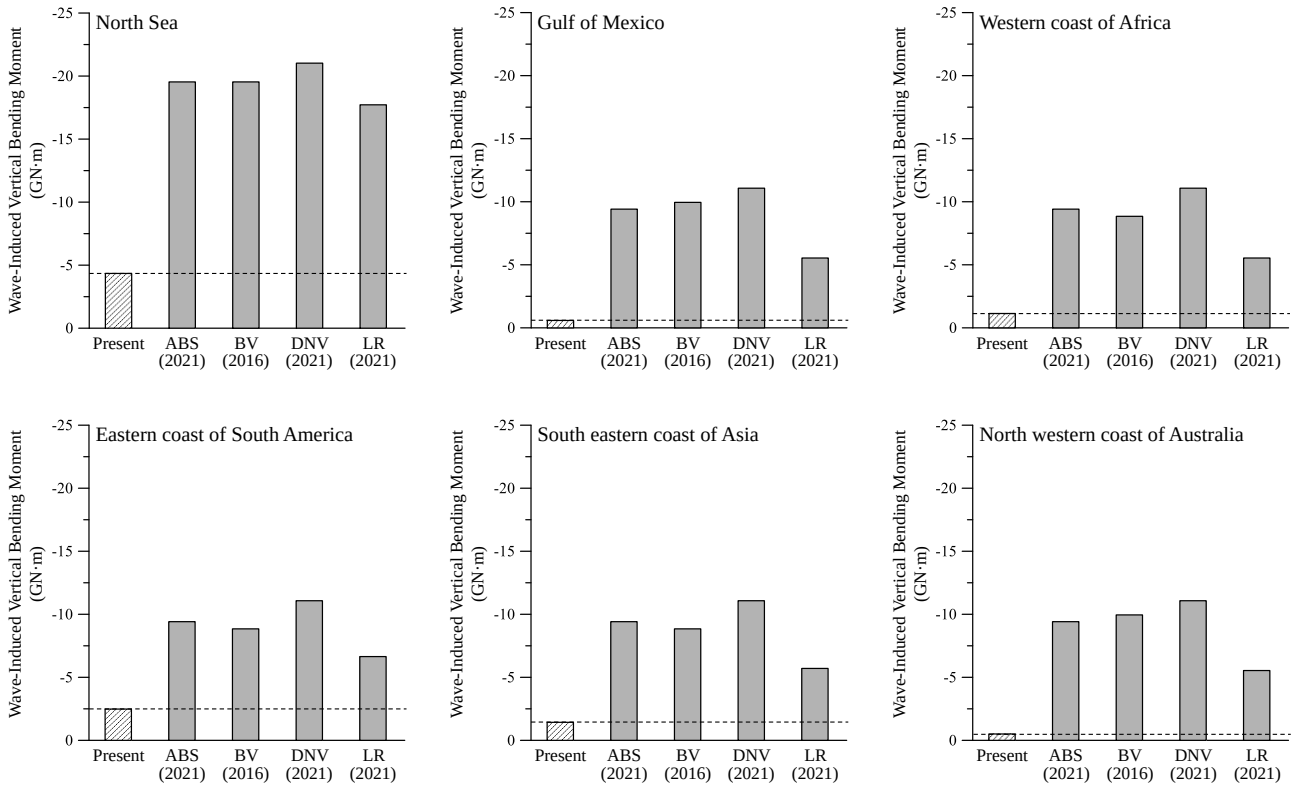

Figure 13. Comparison of the design wave-induced vertical bending moments between the present method (for benign conditions) and classification society rules (for survival conditions) for the six investigated regions

5. CONCLUDING REMARKS

The primary aim of this study was to present a new probabilistic method for determining the design value of wave-induced hull girder loads acting on ship-shaped offshore installations in benign conditions. To demonstrate the proposed method, a hypothetical FPSO model was used to analyse the motion and loads for calculating the wave-induced vertical bending moments. A series of hydrodynamic analyses was performed for the selected credible wave scenarios generated by the LHS technique using best-fit PDFs of the site-specific metocean data.

The results demonstrate that the proposed method is useful for determining the design value of wave-induced hull girder loads for ship-shaped offshore installations in benign conditions corresponding to different site-specific sea states and an acceptable level of exceedance probability. The method can also be used to determine an appropriate mooring system type in terms of wave-induced hull girder loads. A sequel to this paper is ongoing to present a method for determining design values of wave-induced hull girder loads of ship-shaped offshore installations in survival conditions.

6. ACKNOWLEDGEMENTS

This study was undertaken at The Korea Ship and Offshore Research Institute at Pusan National University, South Korea, which has been a Lloyd's Register Foundation Research Centre of Excellence, since 2008. This research was supported by Global Advanced Engineer Education Program for Future Ocean Structure (P0012646) funded by the Ministry of Trade, Industry and Energy. This study was supported by BK21 FOUR Graduate Program for Green-Smart Naval Architecture and Ocean Engineering of Pusan National University.

7. REFERENCES

1. ABS (2021) *Rules for building and classing floating production installation.* American Bureau of Shipping, Houston, TX, USA.
2. ABYANI, M., ASGARIAN, B. & ZARRIN, M. (2018) *Statistical assessment of seismic fragility curves for steel jacket platforms considering global dynamic instability.* Ships and Offshore Structures. 13(4):366-374.
3. BOGGS, D., ENERGY MARITIME ASSOCIATES, BARTON, C., WOOD, ALBAUGH, E.K., P.E. – CONSULTANT & DAVIS, D. (2021) *2021 worldwide survey of floating production, storage and offloading (FPSO) units.* Offshore Magazine, Endeavor Business Media, Houston, Texas, USA.
4. BV (2016) *Rules for the classification of offshore units.* Bureau Veritas, Paris, France.
5. CABRERA-MIRANDA, J.M., SAKUGAWA, P. M., CORONA-TAPIA, R. & PAIK, J.K. (2018) *On design criteria for a disconnectable FPSO*

mooring system associated with expected life-cycle cost. Ships and Offshore Structures. 13:432-442.

6. CAO, Y., YU, X., XIANG, G., RUAN, W. & LU, P. (2018) *On critical parameters of squall associated with the mooring design of a turret-moored FPSO*. Ships and Offshore Structures. 13(S1):S182-S190.
7. CHAKRABARTI, S.K. (2005) *Handbook of offshore engineering (Volume 1)*. Elsevier, London, UK.
8. CHEN, N-Z. (2016) *Hull girder reliability assessment for FPSOs*. Engineering Structures. 114:135-147.
9. DANIEL, J., MASTRANGELO, C. F., GANGULY, P. (2013) *First floating, production storage and offloading vessel in the U.S. Gulf of Mexico*. Offshore Technology Conference 2013, (OTC2013-24112), Houston, Texas, USA. 6-9 May.
10. DHI (2019) *MIKE 21 spectral wave module scientific documentation*. Danish Hydraulic Institute, Hørsholm, Denmark.
11. DNV (2019) *Recommended practice DNV-RP-C205: Environmental conditions and environmental loads*. Det Norske Veritas, Oslo, Norway.
12. DNV (2021) *Offshore standards: Structural design of offshore ship-shaped and cylindrical units*. Det Norske Veritas, Oslo, Norway.
13. FONSECA, N., PASCOAL, R., GUEDES SOARES, C., CLAUSS, G. & SCHMITTNER, C. (2010) *Numerical and experimental analysis of extreme wave induced vertical bending moments on a FPSO*. Applied Ocean Research. 32:374-390.
14. FONTAINE, E., ORSERO, P., LEDOUX, A., NERZIC, R., PREVOSTO, M. & QUINIOU, V. (2013) *Reliability analysis and response based design of a moored FPSO in west Africa*. Structural Safety. 41:82-96.
15. GASPAR, B., TEIXEIRA, A.P. & GUEDES SOARES, C. (2016) *Effect of the nonlinear vertical wave-induced bending moments on the ship hull girder reliability*. Ocean Engineering. 119:193-207.
16. GUEDES SOARES, C., FONSECA, N., PASCOAL, R., CLAUSS, G. F., SCHMITTNER, C. E. & HENNIG, J. (2006) *Analysis of design wave loads on an FPSO accounting for abnormal waves*. Journal of Offshore Mechanics and Arctic Engineering. 128:241-247.
17. HA, S., SEO, S-H., ROH, M-I. & SHIN, H-K. (2016) *Simplified nonlinear model for the weight estimation of FPSO plant topside using the statistical method*. Ships and Offshore Structures. 11(6):603-619.
18. HA, S., UM, T-S., ROH, M-I. & SHIN, H-K. (2017) *A structural weight estimation model of FPSO topsides using an improved genetic programming method*. Ships and Offshore Structures. 12(1):43-55.
19. HAMDAN. F. (2003) *Margins of safety in FPSO hull strength*. Research Report 083. Health and Safety Executive, London, UK.
20. HENRIKSEN, L., KAMISHOHARA, A. & HOSOKAWA, H. (2008) *Structural analysis and modifications-2 tankers for offshore FPSO and FSO service*. Ships and Offshore Structures. 3(2):127-134.
21. HWANG, J-K., ROH, M-I. & LEE, K-Y. (2010) *Detailed design and construction of the hull of a floating, production, storage and off-loading (FPSO) unit*. Ships and Offshore Structures. 5(2):93-104.
22. IACS (2021) *Common structural rules for bulk carriers and oil tankers*. International Association of Classification Societies, London, UK.
23. IVANOV, L.D., KU, A., HUANG, B. & KRZONKALA, V.C.S. (2011) *Probabilistic presentation of the total bending moments of FPSOs*. Ships and Offshore Structures. 6(1-2):45-58.
24. KRISTOFFERSEN, J.C., BREDMOSE, H., GEORGAKIS, C.T., BRANGER, H. & LUNEAU, C. (2021) *Experimental study of the effect of wind above irregular waves on the wave-induced load statistics*. Coastal Engineering. 168:103940.
25. LIU, S., XIAO, L. & KOU, Y. (2016) *Probability analysis and parameter estimation for nonlinear relative wave motions on a semi-submersible using the method of LH-moments*. Ships and Offshore Structures. 11(7):720-733.
26. LR (2021) *Rules and regulations for the classification of offshore units*. Lloyd's Register, London, UK.
27. MA, M., ZHAO, C. & DANEESE, N. (2012) *A method of applying linear seakeeping panel pressure to full ship structural models*. 11th International Conference on Computer Applications and Information Technology in the Maritime Industries, Liege, Belgium. 16-18 April.
28. MAERLI, A., DAS, P. & SMITH, S. (2000) *A rationalization of failure surface equation for the reliability analysis of FPSO structures.* International Shipbuilding Progress. 47:215-225.
29. NUBLI, H. & SOHN, J.M. (2021) *Procedure for determining design accidental loads in liquified-natural-gas-fuelled ships under explosion using a computational-fluid-dynamics-based simulation approach*. Ships and Offshore Structures. DOI: https://doi.org/10.1080/17445302.2021.1983249.
30. OLSEN, A.S., SCHRØTER, C. & JENSEN, J.J. (2006) *Wave height distribution observed by ships in the North Atlantic*. Ships and Offshore Structures. 1(1):1-12.

31. OZGUC, O. (2020) *Conversion of an oil tanker into FPSO in Gulf of Mexico: strength and fatigue assessment*. Ships and Offshore Structures. 16(9):993-1011.
32. PAIK, J.K. (2018) *Ultimate limit state analysis and design of plated structures*. 2nd Ed. John Wiley & Sons, Chichester, UK.
33. PAIK, J.K. (2020) *Advanced structural safety studies with extreme conditions and accidents*. Springer, Singapore.
34. PAIK, J.K. (2022) *Ship-shaped offshore installations: design, construction, operation, healthcare, and decommissioning*. 2nd Ed. Cambridge University Press, Cambridge, UK.
35. PAIK, J.K., LEE, D.H., KIM, S.J., THOMAS, G. & MA, M. (2019) *A new method for determining the design values of wave-induced hull girder loads acting on ships*. Ships and Offshore Structures. 14(S1):63-90.
36. PRINI, F., BENSON, S., BIRMINGHAM, R.W., DOW, R.S., FERGUSON, L.J., SHEPPARD, P.J., PHILLIPS, H.J., JOHNSON, M.C., MEDIAVILLA VARAS, J. & HIRDARIS, S. (2018a) *Full-scale seakeeping trials of an all-weather lifeboat*. The Royal Institution of Naval Architects SURV9 Conference: Surveillance, Pilot & Rescue Craft, ISBN (Electronic) 9781909024755.
37. PRINI, F., BIRMINGHAM, R.W., BENSON, S., DOW, R.S., SHEPPARD, P.J., PHILLIPS, H.J., JOHNSON, M.C., MEDIAVILLA VARAS, J. & HIRDARIS, S. (2018b) *Enhanced structural design and operation of search and rescue craft*. Marine Design XIII, 13th International Marine Design Conference (IMDC 2018), Helsinki, Finland. 10-14 June. 1st Edition, CRC Press: eBook ISBN 9780429440533.
38. RÖRUP, J., DARIE, I. & MACIOLOWSKI, B. (2017) *Strength analysis of ship structures with open decks*. Ships and Offshore Structures. 12(S1):S189-S199.
39. SHA, Y., AMDAHL, J., AALBERG, A. & YU, Z. (2018) *Numerical investigations of the dynamic response of a floating bridge under environmental loading*. Ships and Offshore Structures. 13(S1):S113-S126.
40. SOGSTAD, B.E. (1995) *A sensitivity study of hull girder wave loads for ship shaped oil production and storage vessels*. 27th Offshore Technology Conference, (OTC1995-7769), Houston, Texas, USA. 1-4 May.
41. TANAKA, Y., OGAWA, H., TATSUMI, A. & FUJIKUBO, M. (2015) *Analysis method of ultimate hull girder strength under combined loads*. Ships and Offshore Structures. 10(5):587-598.
42. XU, X., SAHOO, P., EVANS, J. & TAO, Y. (2019) *Hydrodynamic performances of FPSO and shuttle tanker during side-by-side offloading operation*. Ships and Offshore Structures. 14(S1):S292-S299.
43. YE, K.Q. (1998) *Orthogonal column Latin hypercubes and their application in computer experiments*. Journal of the American Statistical Association. 93:1430-1439.
44. YOUSSEF, S.A.M., FAISAL, M., SEO, J.K., KIM, B.J., HA, Y.C., KIM, D.K., PAIK, J.K., CHENG, F. & KIM, M.S. (2016) *Assessing the risk of ship hull collapse due to collision*. Ships and Offshore Structures. 11(4):335-350.
45. ZANGENEH, R., THIAGARAJAN, K.P., URBINA, R. & TIAN, Z. (2017) *Effect of viscous damping on the heading stability of turret-moored tankers*. Ships and Offshore Structures. 12(3):360-369.
46. ZHAO, C. & MA M. (2016) *A hybrid 2.5-dimensional high-speed strip theory method and its application to apply pressure loads to 3-dimensional full ship finite element models*. Journal of Ship Production and Design. 32(4):216-225.
47. ZHAO, C., MA, M. & HUGHES, O.F. (2013) *Applying strip theory based linear seakeeping loads to 3D full ship finite element models*. 32nd International Conference on Ocean, Offshore and Arctic Engineering, (OMAE2013-10124), Nantes, France. 9-14 June.
48. ZHAO, W., YANG, J., HU, Z. & WEI, Y. (2012) *Full-scale measurement investigation of the hydrodynamics of a turret-moored FPSO in a typhoon and deduction of its mooring loads*. Ships and Offshore Structures. 7(3):285-295.
49. ZHAO, Y. & DONG, S. (2020) Design load estimation with IFORM-based models considering long-term extreme response for mooring systems. Ships and Offshore Structures. DOI:https://doi.org/10.1080/17445302.2020.1838118.

